Astronomy & Astrophysics manuscript no. output
April 26, 2021

Pulsating hydrogen-deficient white dwarfs and pre-white dwarfs observed with *TESS*

II. Discovery of two new GW Vir stars: TIC 333432673 and TIC 095332541

Murat Uzundag[1,2], Alejandro H. Córsico[3,4], S. O. Kepler[5], Leandro G. Althaus[3,4], Klaus Werner[6], Nicole Reindl[7], Keaton J. Bell[8,9], Michael Higgins[10], Gabriela O. da Rosa[5], Maja Vučković[1], Alina Istrate[11]

[1] Instituto de Física y Astronomía, Universidad de Valparaíso, Gran Bretaña 1111, Playa Ancha, Valparaíso 2360102, Chile
[2] European Southern Observatory, Alonso de Cordova 3107, Santiago, Chile
[3] Grupo de Evolución Estelar y Pulsaciones. Facultad de Ciencias Astronómicas y Geofísicas, Universidad Nacional de La Plata, Paseo del Bosque s/n, 1900 La Plata, Argentina
[4] IALP - CONICET
[5] Instituto de Física, Universidade Federal do Rio Grande do Sul, 91501-970, Porto-Alegre, RS, Brazil
[6] Institut für Astronomie und Astrophysik, Kepler Center for Astro and Particle Physics, Eberhard Karls Universität, Sand 1,72076 Tübingen, Germany
[7] Institute for Physics and Astronomy, University of Potsdam, Karl-Liebknecht-Str. 24/25, D-14476 Potsdam, Germany
[8] DIRAC Institute, Department of Astronomy, University of Washington, Seattle, WA-98195, USA
[9] NSF Astronomy and Astrophysics Postdoctoral Fellow
[10] Department of Physics, Duke University, Durham, NC-27708, USA
[11] Department of Astrophysics/IMAPP, Radboud University, P O Box 9010, NL-6500 GL Nijmegen, The Netherlands
e-mail: murat.uzundag@postgrado.uv.cl

ABSTRACT

Context. The *TESS* mission is revolutionizing the blossoming area of asteroseismology, particularly of pulsating white dwarfs and pre-white dwarfs, thus continuing the impulse of its predecessor, the *Kepler* mission.
Aims. In this paper, we present the observations from the extended *TESS* mission in both 120 s short-cadence and 20 s ultra-short-cadence mode of two pre-white dwarf stars showing hydrogen deficiency. We identify them as two new GW Vir stars, TIC 333432673 and TIC 095332541. We apply the tools of asteroseismology with the aim of deriving their structural parameters and seismological distances.
Methods. We carried out a spectroscopic analysis and a spectral fitting of TIC 333432673 and TIC 095332541. We also processed and analyzed the high-precision *TESS* photometric light curves of the two target stars, and derived their oscillation frequencies. We performed an asteroseismological analysis of these stars on the basis of PG 1159 evolutionary models that take into account the complete evolution of the progenitor stars. We searched for patterns of uniform period spacings in order to constrain the stellar mass of the stars, and employed the individual observed periods to search for a representative seismological model.
Results. The analysis of the *TESS* light curves of TIC 333432673 and TIC 095332541 reveal the presence of several oscillations with periods ranging from 350 to 500 s associated to typical gravity (g)-modes. From follow-up ground-based spectroscopy, we find that both stars have the similar effective temperature ($T_{\rm eff}$ = 120,000 ± 10,000 K) and surface gravity ($\log g$ = 7.5 ± 0.5) but a slightly different He/C composition of their atmosphere. On the basis of PG 1159 evolutionary tracks, we derived a spectroscopic mass of $M_\star = 0.58^{+0.16}_{-0.08} M_\odot$ for both stars. Our asteroseismological analysis of TIC 333432673 allowed us to find a constant period spacing compatible with a stellar mass $M_\star \sim 0.60 - 0.61 M_\odot$, and an asteroseismological model for this star with a stellar mass $M_\star = 0.589 \pm 0.020\ M_\odot$ and a seismological distance of $d = 421 \pm 120$ pc. We find an excellent agreement between the different inferences of the stellar mass, and also between the seismological distance an that measured with *Gaia* ($d_{\rm Gaia}$ = 389 pc). Unfortunately, we have not been able to put constraints on the stellar mass and distance of TIC 095332541 with our asteroseismological tools.
Conclusions. Using the high-quality data collected by the *TESS* space mission and follow-up spectroscopy, we have been able to discover and characterize two new GW Vir stars. The *TESS* mission is having (and will continue to have) an unprecedented impact on the area of white-dwarf asteroseismology.

Key words. asteroseismology — stars: oscillations (including pulsations) — stars: interiors — stars: evolution — stars: white dwarfs

1. Introduction

GW Vir stars are pulsating PG 1159 stars, that is, pulsating hot hydrogen (H)-deficient, carbon (C)-, oxygen (O)-, helium (He)-rich white dwarf (WD) and pre-WD stars. PG 1159 stars represent the evolutionary link between post-AGB stars and most of the H-deficient WDs, including DO and DB WDs (Werner & Herwig 2006). These stars likely have their origin in a born-again episode induced by a post-AGB He thermal pulse (see Herwig 2001; Blöcker 2001; Althaus et al. 2005; Miller Bertolami et al. 2006, for references). GW Vir stars constitute the hottest class of pulsating WDs and pre-WDs, the other categories being the DAV or ZZ Ceti (H-rich atmospheres) stars, DBV or V777 Her (H-rich atmospheres) stars, ELMV stars (H-rich atmo-

spheres and extremely low masses), and pre-ELMV stars, likely the precursors of the ELMVs (see the reviews by Winget & Kepler 2008; Althaus et al. 2010; Córsico et al. 2019). The category of GW Vir stars includes PNNV stars, which are still surrounded by a nebula, and DOV stars, that lack a nebula (Winget et al. 1991), and also the pulsating Wolf-Rayet central stars of planetary nebula ([WC] stars) and Early-[WC] = [WCE] stars, because they share the same pulsation properties of pulsating PG 1159 stars (Quirion et al. 2007). GW Vir stars exhibit multiperiodic luminosity variations with periods in the range 300–6000 sec, originated by g(gravity)-mode pulsations excited by the κ-mechanism due to partial ionization of C and O in the outer layers[1] (Starrfield et al. 1983, 1984; Stanghellini et al. 1991; Saio 1996; Gautschy 1997; Gautschy et al. 2005; Córsico et al. 2006; Quirion et al. 2007).

Asteroseismology of WDs and pre-WDs has been strongly promoted during the last decade mainly by the availability of space missions that provide unprecedented high-quality data. Particularly, the *Kepler* satellite, both the main mission (Borucki et al. 2010) and the *K2* mode (Howell et al. 2014), allowed the study of 32 ZZ Ceti stars and two V777 Her stars (Østensen et al. 2011; Greiss et al. 2014; Hermes et al. 2014; Bell et al. 2015; Hermes et al. 2017a,b; Bell et al. 2017; Córsico 2020), until it was out of operation by October 2018. The successor of *Kepler* is the Transiting Exoplanet Survey Satellite (*TESS*, Ricker et al. 2015). *TESS* has provided extensive photometric observations of the 200 000 brightest stars in 85 % of the sky in the first part of the mission, each observation with a time base of about 27 days per sector observed. In the context of pulsating WDs and pre-WDs, the high-quality observations of *TESS*, combined with ground-based observations, are able to provide a very important input to the asteroseismology of DBVs (Bell et al. 2019; Bognár et al. 2021), DAVs (Bognár et al. 2020), pre-ELMVs (Wang et al. 2020; Hong et al. 2021), and GW Vir stars (Córsico et al. 2021).

In this work, we report for the first time the photometric variability of the PG1159 stars TIC 333432673 (WD J064115.64−134123.77) and TIC 095332541 (WD J060244.99−135103.57) observed with *TESS*. Given the small number of already known pulsating stars of this class (19 objects; see Córsico et al. 2019), the discovery of two new GW Vir stars constitutes a particularly relevant finding, even more since the *Kepler*/*K2* mission publications do not include any new object of this nature to date. We perform an asteroseismological analysis of these stars based on the state-of-the-art evolutionary models of PG 1159 stars of Althaus et al. (2005) and Miller Bertolami & Althaus (2006). This study is the second part of our series of papers devoted to the study of pulsating H-deficient WDs observed with *TESS*. The first article was devoted to a set of six already known GW Vir stars (Córsico et al. 2021).

The paper is organized as follows. In Sect. 2, we present the details of the spectroscopic observations and the data reduction. In Sect. 3, we derive atmospheric parameters for each star by fitting synthetic spectra to the newly obtained low-resolution spectra. In Sect. 4, we analyse the photometric *TESS* data and give details on the frequency analysis. Sect. 5 is devoted to the asteroseismic analysis of our targets. Finally, in Sect. 6, we summarize our main results.

[1] Due to the high surface temperatures of these stars, it is likely that they do not have convection in their envelopes, making them one of the few classes of pulsating stars for which the well known complication of the convection-pulsation interaction in the pulsational stability analyses is not present.

2. Spectroscopy

TIC 333432673 (WD J064115.64−134123.77) and TIC 095332541 (WD J060244.99−135103.57) were classified as white dwarf candidates by Gentile Fusillo et al. (2019) from their colors and *Gaia* DR2 parallax. The *Gaia* DR3 parallax and corresponding distance for TIC 333432673 are $\pi = 2.57^{+0.07}_{-0.04}$ mas and $d = 389.00^{+5.59}_{-5.22}$ pc, while for TIC 095332541 are $\pi = 2.60^{+0.07}_{-0.04}$ mas and $d = 384.48^{+5.54}_{-5.04}$ pc (Bailer-Jones et al. 2021), respectively. We obtained spectroscopic observations for TIC 333432673 and TIC 095332541, to determine the atmospheric parameters.

TIC 333432673 was observed with the Southern Astrophysical Research (SOAR) Telescope, a 4.1-meter aperture optical and near-infrared telescope (Clemens et al. 2004), situated at Cerro Pachón, Chile on March 5, 2021 (under the program allocated by the Chilean Time Allocation Committee (CNTAC), no:CN2020B-74). We use Goodman spectrograph with a setup of 400 l/mm grating with the blaze wavelength 5500 Å (M1: 3000-7050 Å) with a slit of 1 arcsec. This setup provides a resolution of about 5.6 Å. The data reduction has been partially done by using the instrument pipeline[2] including overscan, trim, slit trim, bias and flat corrections. For cosmic rays identification and removal, we used an algorithm as described by Pych (2004), which is embedded in the pipeline. Then, we applied the wavelength calibrations using the frames obtained with the internal He-Ar-Ne comparison lamp at the same telescope position as the targets. In a last step, we normalized the spectrum with a high-order Legendre function, using the standard star EG 274 observed with the same setup.

TIC 095332541 was observed with the Isaac Newton Telescope (INT), a 2.54 m (100 in) optical telescope run by the Isaac Newton Group of Telescopes at Roque de los Muchachos Observatory on La Palma on February 15 and 16, 2021 (ProgID: ING.NL.21A.003) with an exposure time of 1800 s, respectively. We used the Intermediate Dispersion Spectrograph (IDS) long-slit spectrograph with the grating R400V (R = 1452) and a 1.5 arcsec slit. This setup provides a resolution of about 3.5 Å. Bias and flat field corrections were applied to the data, the wavelength calibration was performed with Cu-Ne-Ar calibration lamp spectra. We did not flux calibrate the spectra. The signal-to-noise ratio (SNR) of the final spectra is around 80 (see Table 1).

3. Spectral fitting

The spectra of both stars exhibit lines exclusively from He II and C IV. Oxygen, which is usually the most abundant element after He and C in PG1159 stars, and nitrogen, which is found as trace element in some PG1159 stars, might be detectable spectra of better resolution and signal-to-noise ratio. There are no hints for the presence of hydrogen in the spectra.

For the spectral analysis, we used a grid of line-blanketed non-local thermodynamic equilibrium (non-LTE) model atmospheres consisting of H, He, and C as introduced by Werner et al. (2014). In essence, it spans $T_{\rm eff}$ = 60,000–140,000 K in effective temperature and $\log g$ = 4.8–8.3 in surface gravity, with steps of 5,000 K or 10,000 K and 0.3 dex, respectively. C/He mass ratios in the range 0.0–1.0 were considered. Synthetic spectra were convolved with a Gaussian accounting for the spectral resolution of the observations. The best fitting models were chosen by visual comparison with the rectified observed spectra.

[2] https://github.com/soar-telescope/goodman_pipeline

Table 1. Log of spectroscopic observations.

TIC	Name	RA (J2000)	Dec (J2000)	Exp. (sec)	S/N (at 4200 Å)	Telescope/Inst.
333432673	WD J064115.64−134123.77	06:41:15.88	-13:41:31.31	450	80	SOAR/GOODMAN
095332541	WD J060244.99−135103.57	06:02:45.00	-13:51:03.50	2x1800	80	INT/IDS

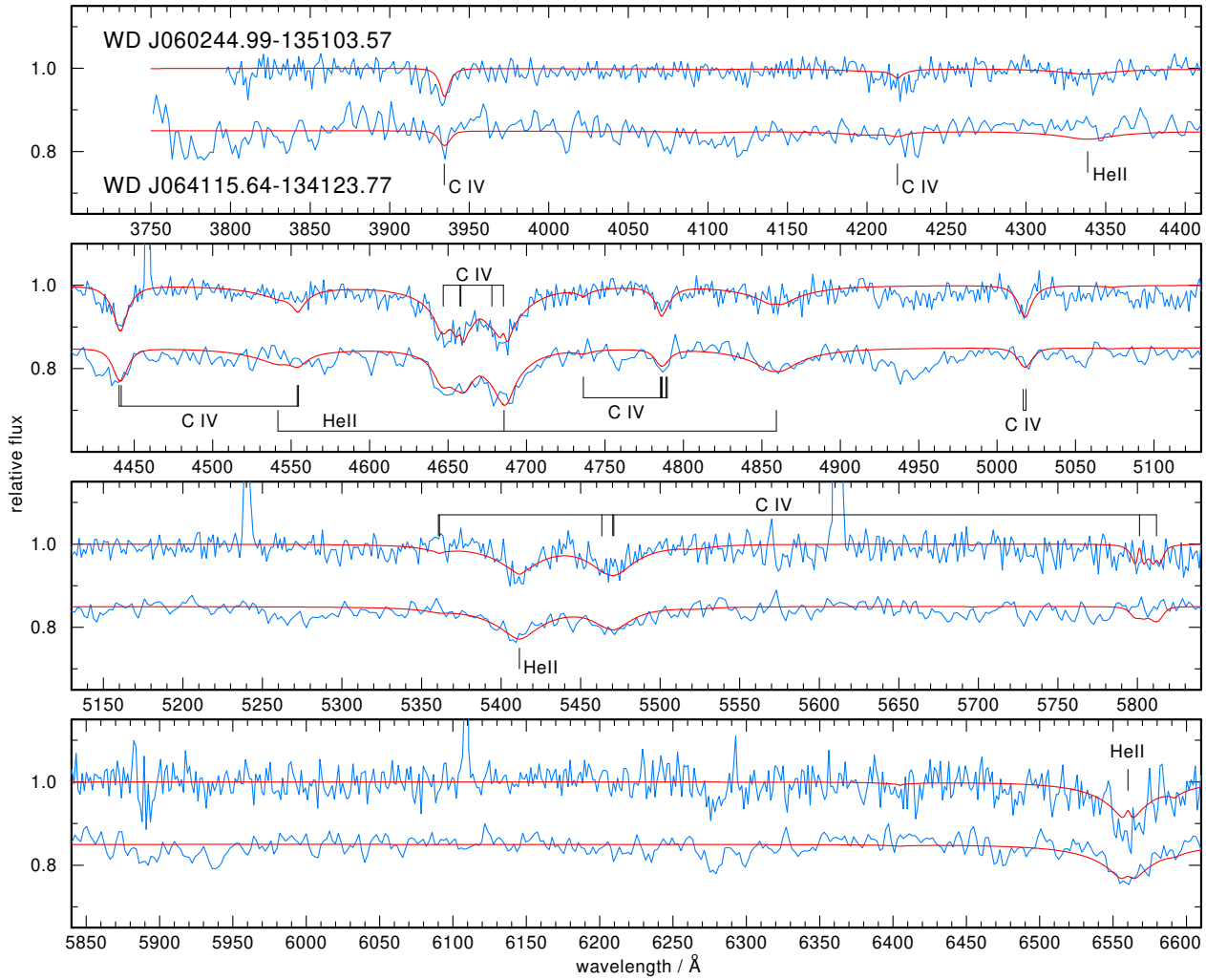

Fig. 1. Optical spectra of the two new GW Vir stars. Overplotted are the best-fit models. Identifications of He II and C IV lines are marked.

The model fits are displayed in Fig. 1. Both stars have $T_{\rm eff}$ = 120,000 ± 10,000 K and $\log g$ = 7.5 ± 0.5, but a different atmospheric composition. For WD J060244.99−135103.57 we found He = $0.50^{+0.20}_{-0.05}$ and C = $0.50^{+0.05}_{-0.20}$ and for WD J064115.64−134123.77 we measured He = $0.75^{+0.05}_{-0.15}$ and C = $0.25^{+0.15}_{-0.05}$ (mass fractions).

4. Photometric observations — *TESS*

We investigate for variability of the two new PG 1159 stars by examining their high-precision photometric observations obtained with *TESS*. TIC 333432673 was observed with 120 s cadence mode, while TIC 095332541 was observed with 120 s and 20 s cadence modes both on Sector 33, between 2020-Dec-17 and 2021-Jan-13. We downloaded the data from the "Barbara A. Mikulski Archive for Space Telescopes" (MAST)[3]. We downloaded the target pixel files (TPFs) of both targets from the MAST archive with the Python package `lightkurve` (Lightkurve Collaboration et al. 2018). The TPFs are examined to determine the amount of crowding and other potential bright sources near the target. The contamination factor is indicated with the keyword `CROWDSAP`, which gives the ratio of the target flux to the total flux in the *TESS* aperture. For each target, we have checked the contamination by looking at the `CROWDSAP` parameter which is listed in Table 2. In the case of TIC 095332541 the `CROWDSAP` value is about 0.8, which implies that ∼ 20% of the total flux measured in the *TESS* aperture comes from other unresolved sources. We have checked for the nearby targets and their brightness. We found 3 nearby objects to TIC 095332541 within 25 arcsec (based on *Gaia* measurements) with G_{mag} of

[3] `http://archive.stsci.edu`

19.5, 20.78 and 20.76. As the differences in magnitude between TIC 095332541 and the nearby objects are larger than 4, we safely confirm that the variation comes from the PG 1159 star. In addition, these nearby objects are beyond the detection limit of *TESS*.

In the case of TIC 333432673, the CROWDSAP value is around 0.15, which means that more than 80% of the flux in the *TESS* aperture comes from the other blended sources. As the contamination from the nearby targets is non-negligible, we considered the proximity and brightness of nearby *Gaia* sources that could contaminate the photometric aperture. In Fig. 2, we show the field of view of *TESS* for TIC 333432673 with the aperture mask. Within the aperture mask that we used to extract the photometry, four other objects along with TIC 333432673 are located. Two of them are fainter than $G_{mag} = 18$ (circles 2 and 5), and thus it is not possible to detect any variation from them with *TESS*. However, the other two targets (circles 3 and 4) are relatively bright, with G_{mag} of 14.7 and 16.4. The origin of the signals has been found using a locator code (Higgins & Bell, in prep.) that produces a light curve and computes its Fourier transform for each pixel in the star's Target Pixel File (TPF). Then it compares the amplitudes and locates the pixel where each signal period has the highest amplitude. We find that the location of maximum power from the four highest signals in Table 3 is most consistent with the position of the PG 1159 source (*Gaia* source_id 2950907725113997312).

The data are in the FITS format which includes all the photometric information, which have been already processed with the Pre-Search Data Conditioning Pipeline (Jenkins et al. 2016) to remove common instrumental trends. From the FITS file, first we have extracted times in barycentric corrected Julian days ("BJD - 245700"), and fluxes ("PDCSAP FLUX"). Afterwards, we removed outliers by applying a running 5σ clipping mask. The fluxes were then normalized by the mean flux.

The final light curves of the target stars are shown in Fig. 3. After detrending the light curves, we calculated their Fourier transforms (FTs) to search for periodic signals. The FT of the resulting light curves are shown in Fig. 4. For pre-whitening, we employed a nonlinear least square (NLLS) method, by simultaneously fitting each pulsation frequency above the 0.1% false-alarm probability (FAP), calculated randomizing the light curve 1000 times and measuring the highest peaks in their Fourier transforms. This iterative process has been done starting with the highest peak, until there is no peak that appears above 0.1% FAP significance threshold. All prewhitened frequencies for both targets are given in Table 3 and 4 including frequencies (periods) and amplitudes with their corresponding errors and the S/N ratio.

In the case of TIC 333432673, we detected 6 peaks, which are located between 2000 μHz and 3000 μHz. Two frequencies at 2015.393 and 2194.806 μHz show significant residuals. For these residuals, we did not produce NLLS fit to extract from the light curves as they can be due to either photon-count noise caused by contamination of the background light in the aperture or amplitude/frequency/phase variations over the length of the data. The frequencies of 2013.329 and 2015.393 μHz can be considered as a rotationally split dipole mode. If we assume that a central azimuthal component $m = 0$ is missing, then the rotation period of TIC 333432673 would be 5.6 d. If $m = +1$ or -1 is missing, then the rotation period of TIC 333432673 would be 2.8 d.

In the case of TIC 095332541, we identified 6 frequencies in the SC data, while we detected 7 frequencies in USC data. The frequencies that located in a similar region as TIC 333432673, between 2200 and 2900 μHz. In table 4, we present the frequency

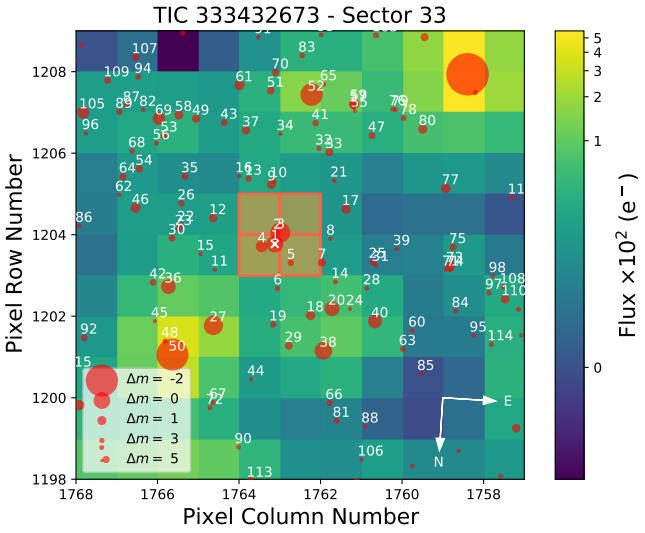

Fig. 2. Target pixel file (TPF) of TIC 333432673 (created with tpfplotter[4], Aller et al. 2020). The aperture mask used by the pipeline to extract the photometry is overplotted with shaded red square. The size of the red circles indicates the Gaia magnitudes of all nearby stars and TIC 333432673 (circle 1 is marked with a cross).

solution that is derived from the USC observations. All frequencies except 2403.783 μHz (f_4) were found also in the FT of SC data. The amplitudes of frequencies that were extracted from USC observations are about 2% higher than the power of the SC observations. This effect can be seen in the lower panel of Fig. 4, where we depicted FT of USC data (orange lines) and the FT of SC data (black lines). We found a doublet for TIC 095332541 as well at 2401.602 and 2403.783 μHz. Again, if we assume that these pattern due to rotational multiplets, then the rotation period of TIC 095332541 would be either 2.65 d (in case of either $m = +1$ or -1 is missing) or 5.3 d (in case of a central azimuthal component $m = 0$ is missing).

The periodicities detected in these two PG 1159 stars are concentrated in a short region from 350 s to 500 s, which agree with the period spectrum typically exhibited by pulsating PG 1159 or GW Vir stars (e.g., McGraw et al. 1979; Winget et al. 1991; Costa et al. 2008; Córsico et al. 2021). Due to the absence of evidence of any nebulae, these two GW Vir stars are classified as DOV stars.

5. Asteroseismology

For the asteroseismological analysis of this work, we employ the set of state-of-the-art evolutionary models of PG 1159 stars of Althaus et al. (2005) and Miller Bertolami & Althaus (2006, 2007a,b). In those works, a set of post-AGB evolutionary sequences computed with the LPCODE evolutionary code (Althaus et al. 2005) were followed through the very late thermal pulse (VLTP) and the resulting born-again episode that give rise to the H-deficient, He-, C- and O-rich composition characteristic of PG 1159 stars. The masses of the resulting remnant models are 0.530, 0.542, 0.565, 0.589, 0.609, 0.664, and 0.741 $M_{\odot}$. In Fig. 5 we show the evolutionary tracks of PG 1159 stars in the $\log T_{\rm eff}$ vs. $\log g$ plane. On the basis of the evolutionary tracks and the values of the spectroscopic surface gravity and effective temperature of TIC 333432673 and TIC 095332541, we derive by interpolation a value of the spectroscopic mass. We obtain a

[4] https://github.com/jlillo/tpfplotter

Table 2. The two new GW Vir stars reported from *TESS* observations, including the name of the targets, *Gaia* magnitude, observed sectors, date, *CROWDSAP* estimate, and length of the runs (columns 1, 2, 3, 4, 5 and 6, respectively). From the Fourier Transform of the original and shuffled data, three different set of parameters: resolution, average noise level of amplitude spectra, and detection threshold which we define as the amplitude at 0.1% false alarm probability, FAP, are presented in columns 7, 8 and 9, respectively. The *CROWDSAP* keyword shows the ratio of the target flux to the total flux in the optimal *TESS* light curve aperture, taking into account that the TESS pixels are 21x21 arcsecs.

Name	$G_{\rm mag}$	Obs. Sector	Start Time (BJD-2 457 000)	CROWDSAP	Length [d]	Resolution μHz	Average Noise Level [ppt]	0.1% FAP [ppt]
TIC 333432673	15.66	33	2201.7372	0.14	25.83	0.45	0.95	3.67
TIC 095332541	15.79	33	2201.7373	0.78	25.83	0.45	0.71	3.06

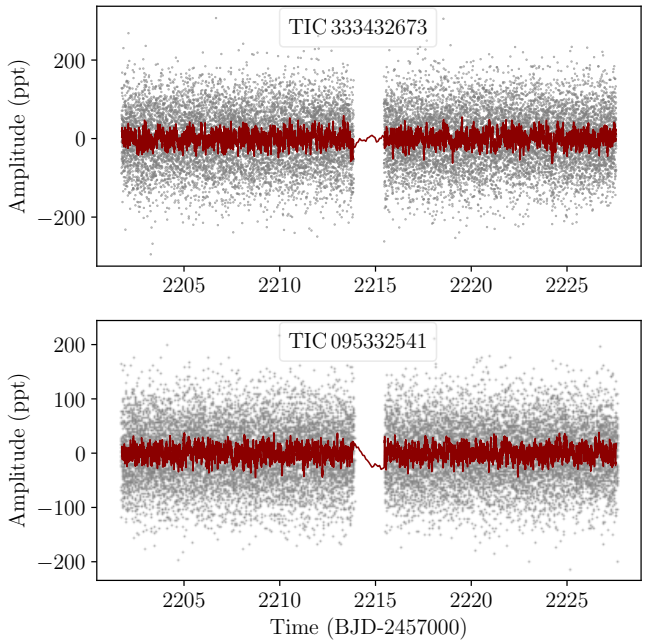

Fig. 3. The light curves of the new pulsating DOV stars TIC 333432673 (upper panel) and TIC 095332541 (lower panel). The red lines are binned light curves which are calculated by running mean every 20 points (corresponding to 38 minutes).

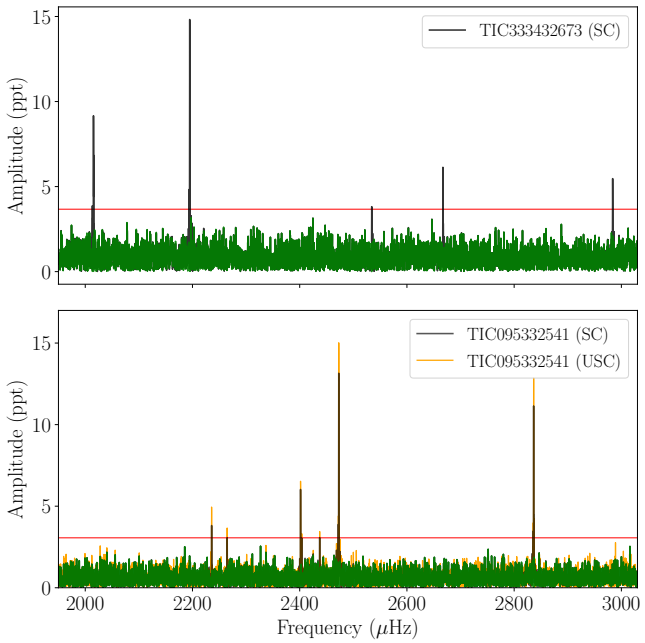

Fig. 4. The FT of the new pulsating DOV stars TIC 333432673 (upper panel) and TIC 095332541 (lower panel). For TIC 095332541, we overplotted both FT of SC (black lines) and USC (orange lines). The horizontal red line indicates the 0.1% FAP level. The green line is the FT of the prewhitened light curve.

Table 3. Independent frequencies, periods, and amplitudes, their uncertainties, and the signal-to-noise ratio in the data of TIC 333432673. Errors are given in parenthesis to 2 significant digits.

Peak	ν (μHz)	Π (s)	A (ppt)	S/N
f_1	2013.329 (44)	496.689 (10)	4.155 (75)	4.38
f_2	2015.393 (23)	496.181 (05)	8.718 (77)	9.19
f_3	2194.806 (15)	455.621 (03)	15.819 (80)	16.68
f_4	2534.342 (47)	394.579 (07)	3.829 (75)	4.03
f_5	2667.136 (29)	374.933 (04)	6.143 (75)	6.48
f_6	2983.709 (33)	335.153 (03)	5.478 (75)	5.77

Table 4. Independent frequencies, periods, and amplitudes, their uncertainties, and the signal-to-noise ratio in the data of TIC 095332541. Errors are given in parenthesis to 2 significant digits.

Peak	ν (μHz)	Π (s)	A (ppt)	S/N
f_1	2235.669 (27)	447.293 (55)	4.975 (57)	7.10
f_2	2264.722 (37)	441.555 (72)	3.675 (57)	5.25
f_3	2401.602 (21)	416.389 (37)	6.447 (57)	9.21
f_4	2403.783 (44)	416.011 (77)	3.105 (57)	4.43
f_5	2437.256 (38)	410.298 (64)	3.578 (57)	5.11
f_6	2472.863 (09)	404.390 (15)	15.119 (57)	21.59
f_7	2836.338 (11)	352.567 (13)	12.856 (57)	18.36

stellar mass of $M_\star = 0.58^{+0.16}_{-0.08}\ M_\odot$ for both GW Vir stars. The large uncertainties of the spectroscopic mass come mainly from the uncertainties in the surface gravity.

In the asymptotic limit of stellar pulsations, i.e., for large radial orders ($k \gg \ell$), g modes of consecutive radial order in WDs and pre-WDs are approximately uniformly spaced in period (Tassoul et al. 1990). The asymptotic period spacing is given by $\Delta\Pi^{\rm a}_\ell = \Pi_0/\sqrt{\ell(\ell+1)}$, $\Delta\Pi^{\rm a}_\ell$ being Π_0 a constant defined as $\Pi_0 = 2\pi^2\left[\int_{r_1}^{r_2}\frac{N}{r}dr\right]^{-1}$, where N is the Brunt-Väisälä frequency (see, e.g., Unno et al. 1989, for its definition). This asymptotic formula constitutes a very precise description of the pulsational properties of chemically homogeneous stellar models, although the g-mode period spacings in chemically stratified PG 1159 stars show appreciable departures from uniformity caused by

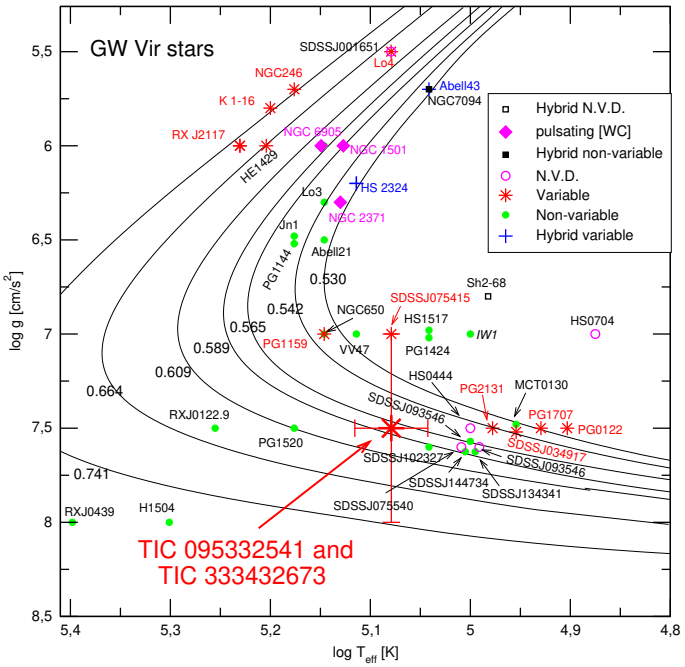

Fig. 5. The already known variable and non-variable PG 1159 stars and variable [WCE] stars in the $\log T_{\rm eff} - \log g$ plane. Thin solid curves show the post-born again evolutionary tracks from Miller Bertolami & Althaus (2006) for different stellar masses. The location of the two new GW Vir stars TIC 333432673 and TIC 095332541 is emphasized with a large red star symbol with error bars. Both stars share the same spectroscopic surface parameters, $T_{\rm eff} = 120\,000 \pm 10\,000$ K and $\log g = 7.5 \pm 0.5$.

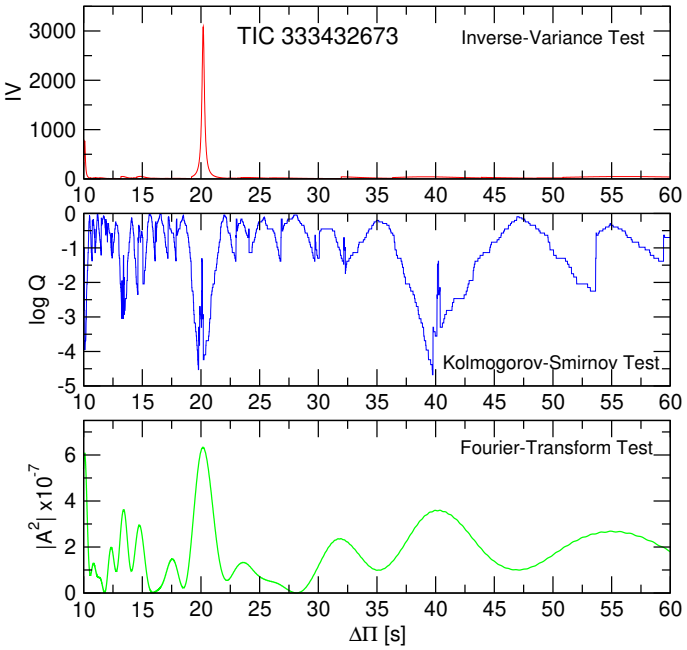

Fig. 6. I-V (upper panel), K-S (middle panel), and F-T significance tests to search for a constant period spacing in TIC 333432673. The tests are applied to the set of 6 pulsation periods of Table 3. A strong signal of a constant period spacing at ~ 20 s is evident. See text for details.

the mechanical resonance called "mode trapping" (Kawaler & Bradley 1994). The observed *average* period spacing of GW Vir stars primarily depends on the stellar mass and the effective temperature (Kawaler & Bradley 1994). It allows us to estimate $M_\star$ by fixing $T_{\rm eff}$. Specifically, a way to derive an estimate of the stellar mass is by comparing the observed average period spacing ($\Delta\Pi$) of the target star with the asymptotic period spacing ($\Delta\Pi^{\rm a}_\ell$) computed at the effective temperature of the star (see the pioneer works of Kawaler 1987, 1988). Since GW Vir stars generally do not have all of their pulsation modes in the asymptotic regime, there is usually no perfect agreement between $\Delta\Pi$ and $\Delta\Pi^{\rm a}_\ell$. A variation of this approach is to compare $\Delta\Pi$ with the *average* of the computed period spacings ($\overline{\Delta\Pi_k}$), instead the asymptotic period spacing.

We searched for a constant period spacing in the data of the new GW Vir stars using the Kolmogorov-Smirnov (K-S; Kawaler 1988), the inverse variance (I-V; O'Donoghue 1994), and the Fourier Transform (F-T; Handler et al. 1997) significance tests. In Fig. 6 we show the results of applying these tests to the set of 6 periods of TIC 333432673 (Table 3). A very strong signature of a period spacing of ~ 20 s is evident according to the three tests. There is also an indication of a possible period spacing of ~ 40 s according to the K-S and F-T tests, although it is completely absent in the I-V test. In Fig. 7 we show the dipole ($\ell = 1$, upper panel) and quadrupole ($\ell = 2$, lower panel) average of the computed period spacings, $\overline{\Delta\Pi_k}$, assessed in a range of periods that includes the periods observed in TIC 095332541 and TIC 333432673 (300 − 500 s), shown as curves for different stellar masses. The g-mode adiabatic pulsation periods employed to assess $\overline{\Delta\Pi_k}$ were computed with the LP-PUL pulsation code (Córsico & Althaus 2006). We can safely discard a period spacing of ~ 40 due to the fact that if such a long period spacing were real, TIC 333432673 should have an extremely low mass, irreconcilable with the spectroscopic mass. Thus, we can assume that the mean period spacing of 20.19 s is robust and reliable for this star. It can be associated with a sequence of $\ell = 1$ modes[5]. We compared this period spacing with the $\overline{\Delta\Pi_k}$ in terms of $T_{\rm eff}$ for all the masses considered in the upper panel of Fig. 7. The resulting mass value is $M_\star \sim 0.61 M_\odot$ or $M_\star \sim 0.60 M_\odot$ if the star is before or after the evolutionary knee, respectively. These values are in good agreement with the spectroscopic mass value ($M_\star = 0.58^{+0.16}_{-0.08}\ M_\odot$).

In Fig. 8 we show the results of applying the significance tests to the set of 6 periods of TIC 095332541 (Table 4). The three tests point to the existence of a probable constant period spacing of $\Delta\Pi \sim 31$ s. If we want to guess what the stellar mass corresponding to this period spacing would be by comparing it with the average of the computed period spacings, we realize that we cannot draw the location of TIC 095332541 in the diagrams of Fig. 7. A period spacing as long as ~ 31 s for TIC 095332541 does not make physical sense, since it would be compatible with a star with unusually low mass (much below $0.4 M_\odot$), in strong conflict with the spectroscopic mass. Therefore, this possible period spacing has to be disregarded. For the same reason, we also rule out a possible period spacing of ~ 45 s that can be seen in Fig. 8. A third possible constant period separation is ~ 13 s, as suggested by the K-S test. Such a short period spacing could make any sense only if all the modes exhibited are quadrupole ($\ell = 2$) modes. In this case, the stellar mass would be $\sim 0.55 M_\odot$ (see lower panel of Fig. 7). However, since this possible period-spacing signature is only suggested by one of the significance tests, we cannot take it as true, and we are forced to discard it. We conclude that it is not possible to find a realistic period spac-

[5] If they were $\ell = 2$, then the stellar mass of TIC 333432673 would be extremely low (see lower panel of Fig. 7), and thus, incompatible with the spectroscopic mass.

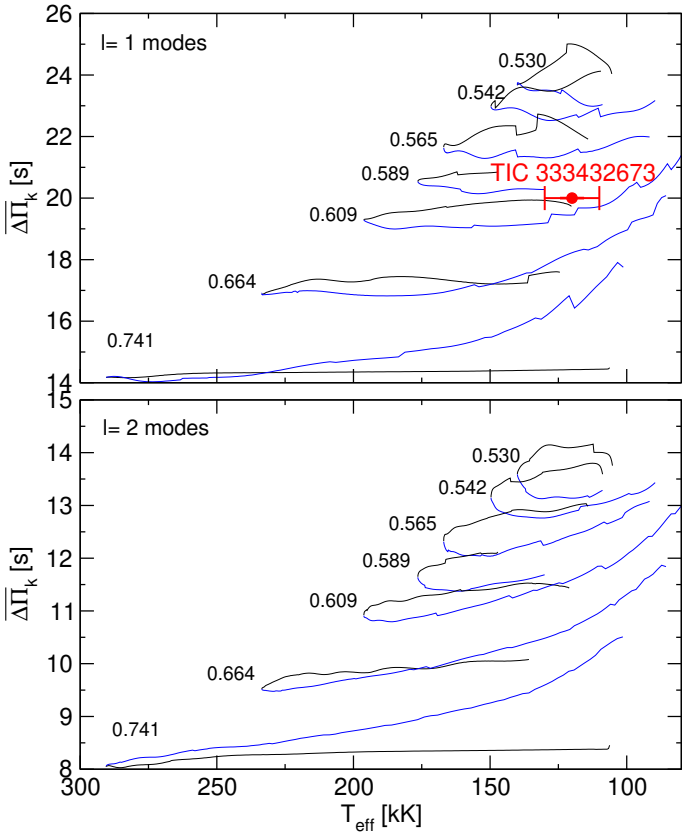

Fig. 7. Upper panel: dipole ($\ell = 1$) average of the computed period spacings, $\overline{\Delta\Pi_k}$, assessed in a range of periods that includes the periods observed in the GW Vir star TIC 095332541 and TIC 333432673, shown as black (blue) curves corresponding to stages before (after) the maximum $T_{\rm eff}$ for different stellar masses. The location of TIC 333432673 when we use the spectroscopic effective temperature, $T_{\rm eff} = 120\,000 \pm 10\,000$ K, and the dipole period spacing $\Delta\Pi_{\ell=1} = 20.19$ s, is highlighted with a red circle. The GW Vir star TIC 09533254 cannot be drawn in this plot if its period spacing is ~ 31 s (see the text). Lower panel: same as in upper panel, but for the average of the computed period spacings with $\ell = 2$.

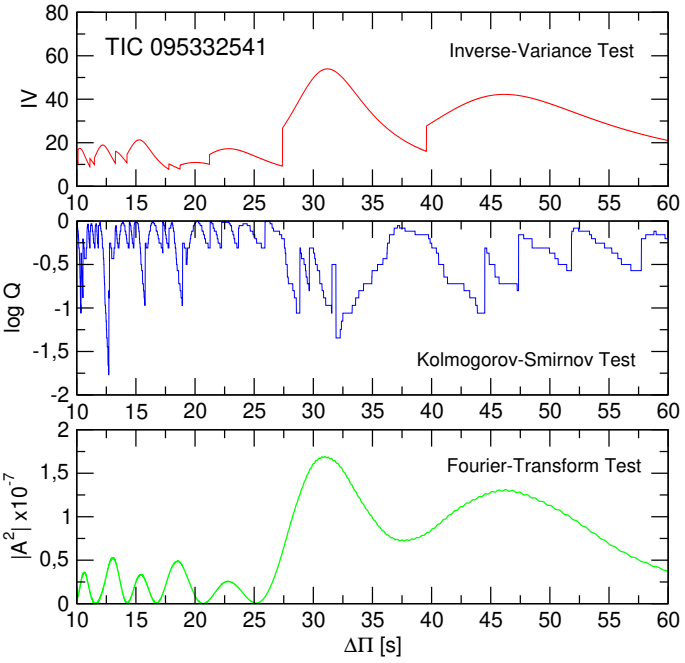

Fig. 8. I-V (upper panel) and K-S (middle panel), and F-T (bottom panel) significance tests to search for a constant period spacing in TIC 095332541, applied to the set of 6 pulsation periods of Table 4. A signal of a constant period spacing at ~ 31 s is evident in the three tests. See text for details.

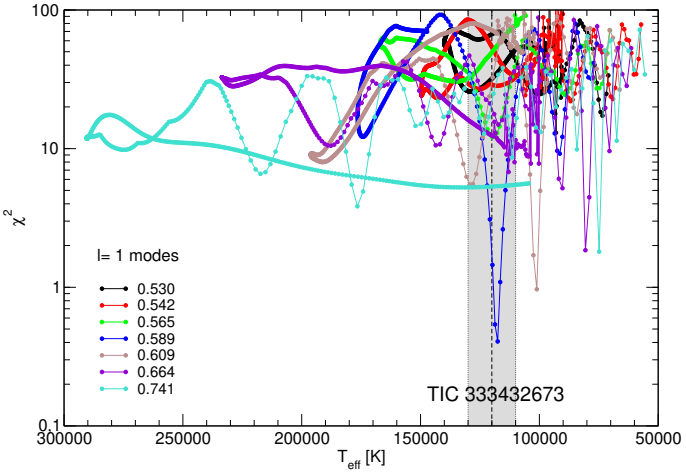

Fig. 9. The quality function of the period fits in terms of the effective temperature for the PG 1159 sequences with different stellar masses (in solar units). We note the presence of a strong minimum corresponding to $M_\star = 0.589 M_\odot$ and $T_{\rm eff} = 117\,560$ K. The vertical dashed line is the spectroscopic $T_{\rm eff}$ of TIC 333432673 (120 000 K) and the gray zone depicts its uncertainties (±10 000 K).

ing for TIC 095332541 with this data set only. This prevents us from estimating its stellar mass and putting constraints on the harmonic degree ℓ of its observed modes.

A powerful asteroseismological tool to disentangle the internal structure of GW Vir stars is to seek theoretical models that best match the individual pulsation periods of the target stars. To measure the goodness of the match between the theoretical pulsation periods ($\Pi_{\ell,k}$) and the observed individual periods ($\Pi_i^{\rm o}$), we assess the merit function $\chi^2(M_\star, T_{\rm eff}) = \frac{1}{N}\sum_{i=1}^{N} \min[(\Pi_{\ell,k} - \Pi_i^{\rm o})^2]$ (see, for instance, Córsico et al. 2021). Here, N is the number of observed periods. In order to find the stellar model that best replicates the observed periods exhibited by each target star — the "asteroseismological" model — we evaluate the function χ^2 for stellar masses between 0.530 and $0.741 M_\odot$ and effective temperatures in the range 80 000 – 300 000 K, with $\Delta T_{\rm eff} \sim 30$ K. For each target star, the PG 1159 model that shows the lowest value of χ^2 is adopted as the best-fit asteroseismological model.

The period-to-period fits for TIC 333432673 lead us to an excellent seismological solution for this star. The quality function corresponding to modes with $\ell = 1$ versus the effective temperature for the different stellar masses is shown in Fig. 9. Among the periods 496.181 s and 496.689 s[6], we have retained only the largest amplitude one, that is, 496.689 s. It is noteworthy the existence of a very clear minima of the quality function ($\chi^2 = 0.407$ s^2) corresponding to an asteroseismological model characterized by an effective temperature of $T_{\rm eff} = 117\,560$ K, very close to the spectroscopic effective temperature of TIC 333432673 and well within its uncertainties ($T_{\rm eff} = 120\,000 \pm 10\,000$ K). The stellar mass of this model is $M_\star = 0.589 M_\odot$, in perfect agreement with the mass derived

[6] These two very close periods could be part of a rotational frequency triplet; see at the end of Sect. 4.

Table 5. Observed and theoretical periods of the asteroseismological model for TIC 333432673 [$M_\star = 0.589 M_\odot$, $T_{\rm eff} = 117\,560$ K, $\log(L_\star/L_\odot) = 1.896$]. Periods are in seconds and rates of period change (theoretical) are in units of 10^{-12} s/s. $\delta\Pi_i = \Pi_i^{\rm O} - \Pi_k$ represents the period differences, ℓ the harmonic degree, and k the radial order.

$\Pi_i^{\rm O}$ (s)	$\ell^{\rm O}$	Π_k (s)	ℓ	k	$\delta\Pi_k$ (s)	$\dot{\Pi}_k$ (10^{-11} s/s)
335.153	1	335.306	1	14	−0.153	6.006
374.933	1	374.215	1	16	0.718	6.763
394.579	1	396.035	1	17	−1.456	5.165
455.621	1	455.941	1	20	−0.320	5.632
496.181	1	496.467	1	22	−0.286	8.181

with the period spacing, $M_\star = 0.60 - 0.61 M_\odot$, and the spectroscopic mass value, $M_\star = 0.58 M_\odot$. We have also performed period fits assuming a mix of $\ell = 1$ and $\ell = 2$ periods, and find the same asteroseismic solution (and with the same value of χ^2). In Table 5 we show a detailed comparison of the observed periods of TIC 333432673 and the theoretical periods of the asteroseismological model. According to our asteroseismological model, all the periods exhibited by the star correspond to $\ell = 1$ modes with high radial order k. We compute the average of the absolute period differences, $\overline{\delta\Pi_i} = \left(\sum_{i=1}^{n} |\delta\Pi_i|\right)/n$, where $\delta\Pi_i = (\Pi_{\ell,k} - \Pi_i^{\rm o})$ and $n = 5$, and the root-mean-square residual, $\sigma = \sqrt{(\sum_{i=1}^{n} |\delta\Pi_i|^2)/n} = \sqrt{\chi^2}$. We compute also the Bayes Information Criterion (BIC; Koen & Laney 2000), BIC $= n_{\rm p}\left(\frac{\log n}{n}\right) + \log\sigma^2$, where $n_{\rm p}$ is the number of free parameters of the models, and n is the number of fitted periods. The smaller the value of BIC, the better the quality of the fit. In our case, $n_{\rm p} = 2$ (stellar mass and effective temperature), and $n = 5$. We obtain $\overline{\delta\Pi_i} = 0.59$ s, $\sigma = 0.75$ s, and BIC $= 0.03$, which means that our period fit is excellent, although admittedly, the differences between theoretical and observed periods is larger than the uncertainties in the measured periods.

We also include in Table 5 the rates of period change ($\dot{\Pi} \equiv d\Pi/dt$) predicted for each g mode of TIC 333432673. Note that all of them are positive ($\dot{\Pi} > 0$), implying that the periods are lengthening over time. The rate of change of periods in WDs and pre-WDs is related to $\dot{T}$ (T being the temperature at the region of the period formation) and $\dot{R}_\star$ ($R_\star$ being the stellar radius) through the order-of-magnitude expression $(\dot{\Pi}/\Pi) \approx -a\,(\dot{T}/T) + b\,(\dot{R}_\star/R_\star)$ (Winget et al. 1983). According to our asteroseismological model, the star is cooling at almost constant radius after reaching its maximum temperature (evolutionary knee), i.e., TIC 333432673 is in its cooling stage. As a consequence, $\dot{T} < 0$ and $\dot{R}_\star \sim 0$, and then, $\dot{\Pi} > 0$. Continuous monitoring of this star could in the future make it possible to measure rates of period change for comparison with our theoretical predictions, if the pulsations are shown to be otherwise coherent over the span of observations.

In Table 6, we list the spectroscopic and astrometric parameters of TIC 333432673 and the main characteristics of the asteroseismological model found in this work. The seismological stellar mass is in excellent agreement with the value derived from the period spacing ($0.60 - 061 M_\odot$) and the spectroscopic mass. The average of the dipole ($\ell = 1$) period spacings of our asteroseismological model is $\overline{\Delta\Pi} = 20.469$ s, in excellent agreement with the $\ell = 1$ mean period spacing derived for TIC 333432673, $\Delta\Pi = 20.19$ s.

Table 6. The main characteristics of the new GW Vir star TIC 333432673. The second column corresponds to spectroscopic results, whereas the third column present results from the asteroseismological model.

Quantity	Spectroscopy Astrometry	Asteroseismology
$T_{\rm eff}$ [kK]	120 ± 10	117.56 ± 12
$M_\star$ [$M_\odot$]	$0.58^{+0.16}_{-0.08}$	0.589 ± 0.020
$\log g$ [cm/s^2]	7.5 ± 0.5	$7.55^{+0.52}_{-0.55}$
$\log(L_\star/L_\odot)$	...	$1.90^{+0.25}_{-0.34}$
$\log(R_\star/R_\odot)$	...	$-1.67^{+0.22}_{-0.25}$
$(X_{\rm He}, X_{\rm C}, X_{\rm O})_{\rm s}$	0.75, 0.25, ⋯	0.30, 0.38, 0.23
d [pc]	$389.56^{+5.59\,(a)}_{-5.22}$	421 ± 120
π [mas]	$2.57^{+0.07\,(a)}_{-0.04}$	$2.38^{+0.94}_{-1.85}$

References: (a) *Gaia*.

We can assess the asteroseismological distance on the basis of the luminosity of the asteroseismological model [$\log(L_\star/L_\odot) = 1.90^{+0.25}_{-0.34}$]. Using a bolometric correction $BC = -7.05$ (extrapolated from the value corresponding to PG 1159035 as given by Kawaler & Bradley 1994), the visual absolute magnitude can be assessed as $M_{\rm V} = M_{\rm B} - BC$, where $M_{\rm B} = M_{\rm B,\odot} - 2.5\,\log(L_\star/L_\odot)$. We employ the solar bolometric magnitude $M_{\rm B\odot} = 4.74$ (Cox 2000). The seismological distance d is derived from the relation: $\log d = 15\,[m_{\rm V} - M_{\rm V} + 5 - A_{\rm V}(d)]$, where we employ the interstellar extinction law of Chen et al. (1998). The interstellar absorption $A_{\rm V}(d)$ is a nonlinear function of the distance and also depends on the Galactic latitude (b). For the equatorial coordinates of TIC 333432673 (Epoch B2000.00, $\alpha = 6^{\rm h}41^{\rm m}15.^{\rm s}88$, $\delta = -13°41'31.''31$) the corresponding Galactic latitude is $b = -7°19'3.''53$. We use the apparent visual magnitude $m_{\rm V} = 15.658$ (*TESS* catalog), and obtain the seismological distance and parallax $d = 421 \pm 120$ pc and $\pi = 2.38^{+0.94}_{-1.85}$ mas, respectively, being the extinction coefficient $A_{\rm V} = 0.50 \pm 0.11$. The large uncertainty in the seismological distance comes mainly from the large uncertainty in the luminosity of the asteroseismological model. A very important check for the validation of the asteroseismological model of TIC 333432673 is the comparison of the seismological distance with the distance derived from astrometry. We have available the estimates from *Gaia*, $d_{\rm G} = 406.56 \pm 9.7$ pc and $\pi_{\rm G} = 2.5 \pm 0.1$ mas. They are in excellent agreement with the asteroseismological derivations in view of the uncertainties in both determinations. This adds confidence to the correctness of the asteroseismological model.

We have also performed period fits for the new GW Vir star TIC 095332541. Unfortunately, our period-to-period fits for this star, either considering all modes as $\ell = 1$, as $\ell = 2$, or as a mixture of $\ell = 1$ and $\ell = 2$, do not allow us to find a clear seismological solution, that is, a single minima of the function χ^2 distinguishable from a crowd of similar minima associated to different effective temperatures and stellar masses. Therefore, we cannot find an asteroseismological model for this star, preventing us from inferring its structural parameters and seismological distance, as we have done for TIC 333432673.

6. Summary and conclusions

In this paper, we have presented the discovery of two new GW Vir stars, TIC 333432673 and TIC 095332541. We have derived atmospheric parameters for both stars by fitting synthetic spectra to the newly obtained low to intermediate resolution SOAR/GOODMAN for TIC 333432673 and INT/IDS for

TIC 095332541 spectra. The determined atmospheric parameters show that TIC 333432673 and TIC 095332541 are identical in terms of surface temperature and surface gravity ($T_{\rm eff}$ = 120,000 ± 10,000 K and $\log g = 7.5 \pm 0.5$) and they are only different regarding the surface C and He abundance.

We investigate the potential variability of the two new PG 1159 stars by examining their short and ultra-short-cadence single-sector observations obtained with *TESS*. Our frequency analysis reveals six significant independent oscillation frequencies for TIC 333432673 and seven for TIC 095332541, which we associate with g-modes. TIC 333432673 exhibits a possible contamination by other sources in the *TESS* aperture within a magnitude limit of $\Delta m = 2$. We examined the target pixel files of TIC 333432673 in order to verify the frequencies that are originated by the PG 1159. We found that the location of the 4 frequencies (S/N $\geq$ 5) is most consistent with the position of TIC 333432673. TIC 333432673 is a great target for ground-based time-series photometry in order to confirm *TESS* signals.The periodicities detected in these two PG 1159 stars are compatible with the period spectrum typically exhibited by GW Vir stars.

We have carried out an asteroseismological investigation on both GW Vir stars employing fully evolutionary models of PG 1159 stars. For TIC 095332541 we have not been able to find a constant period spacing, and therefore it was not possible to derive a stellar mass based on that quantity. Also, we did not find an asteroseismological model for this star, which prevented us from estimating its structural parameters and its seismological distance. On the contrary, for TIC 333432673 we have been able to find a very clear constant period spacing that leads to a stellar mass in very good agreement with the spectroscopic mass. Also for this star, we were able to find an asteroseismological model whose mass is in excellent agreement with the spectroscopic mass, and the derived seismological distance is in concordance with the distance estimated by *Gaia* for this star.

In this paper, we have discovered and characterized two new GW Vir stars using the high-quality data collected by the *TESS* space mission and follow-up spectroscopy. So far, the TESS mission has met the expectations of researchers both in the goal of finding new planetary systems, and in terms of new findings in the area of stellar seismology. We are confident that this mission will continue to provide exciting new discoveries in the field of pulsating WD and pre-WD asteroseismology.

Acknowledgements. M.U. acknowledges financial support from CONICYT Doctorado Nacional in the form of grant number No: 21190886 and ESO studentship program. SOK is supported by CNPq-Brazil, CAPES-Brazil and FAPERGS-Brazil. K.J.B. is supported by the National Science Foundation under Award AST-1903828. This paper includes data collected with the TESS mission, obtained from the MAST data archive at the Space Telescope Science Institute (STScI). Funding for the TESS mission is provided by the NASA Explorer Program. STScI is operated by the Association of Universities for Research in Astronomy, Inc., under NASA con-tract NAS 5–26555. Part of this work was supported by AGENCIA through the Programa de Modernización Tecnológica BID 1728/OC-AR, and by the PIP 112-200801-00940 grant from CONICET. This research has made use of NASA's Astrophysics Data System. Financial support from the National Science Centre under projects No. UMO-2017/26/E/ST9/00703 and UMO-2017/25/B/ST9/02218 is appreciated.

References

Aller, A., Lillo-Box, J., Jones, D., Miranda, L. F., & Barceló Forteza, S. 2020, A&A, 635, A128
Althaus, L. G., Córsico, A. H., Isern, J., & García-Berro, E. 2010, A&A Rev., 18, 471
Althaus, L. G., Serenelli, A. M., Panei, J. A., et al. 2005, A&A, 435, 631
Bailer-Jones, C. A. L., Rybizki, J., Fouesneau, M., Demleitner, M., & Andrae, R. 2021, VizieR Online Data Catalog, I/352
Bell, K. J., Córsico, A. H., Bischoff-Kim, A., et al. 2019, A&A, 632, A42
Bell, K. J., Hermes, J. J., Bischoff-Kim, A., et al. 2015, The Astrophysical Journal, 809, 14
Bell, K. J., Hermes, J. J., Vanderbosch, Z., et al. 2017, ApJ, 851, 24
Blöcker, T. 2001, Ap&SS, 275, 1
Bognár, Z., Kalup, C., & Sódor, Á. 2021, arXiv e-prints, arXiv:2103.17192
Bognár, Z., Kawaler, S. D., Bell, K. J., et al. 2020, A&A, 638, A82
Borucki, W. J., Koch, D., Basri, G., et al. 2010, Science, 327, 977
Chen, B., Vergely, J. L., Valette, B., & Carraro, G. 1998, A&A, 336, 137
Clemens, J. C., Crain, J. A., & Anderson, R. 2004, in Society of Photo-Optical Instrumentation Engineers (SPIE) Conference Series, Vol. 5492, Ground-based Instrumentation for Astronomy, ed. A. F. M. Moorwood & M. Iye, 331–340
Córsico, A. H. 2020, Frontiers in Astronomy and Space Sciences, 7, 47
Córsico, A. H. & Althaus, L. G. 2006, A&A, 454, 863
Córsico, A. H., Althaus, L. G., & Miller Bertolami, M. M. 2006, A&A, 458, 259
Córsico, A. H., Althaus, L. G., Miller Bertolami, M. M., & Kepler, S. O. 2019, A&A Rev., 27, 7
Córsico, A. H., Uzundag, M., Kepler, S. O., et al. 2021, A&A, 645, A117
Costa, J. E. S., Kepler, S. O., Winget, D. E., et al. 2008, A&A, 477, 627
Cox, A. N. 2000, Allen's astrophysical quantities
Gautschy, A. 1997, A&A, 320, 811
Gautschy, A., Althaus, L. G., & Saio, H. 2005, A&A, 438, 1013
Gentile Fusillo, N. P., Tremblay, P.-E., Gänsicke, B. T., et al. 2019, MNRAS, 482, 4570
Greiss, S., Gänsicke, B. T., Hermes, J. J., et al. 2014, MNRAS, 438, 3086
Handler, G., Pikall, H., O'Donoghue, D., et al. 1997, MNRAS, 286, 303
Hermes, J. J., Charpinet, S., Barclay, T., et al. 2014, ApJ, 789, 85
Hermes, J. J., Gänsicke, B. T., Kawaler, S. D., et al. 2017a, ApJS, 232, 23
Hermes, J. J., Kawaler, S. D., Bischoff-Kim, A., et al. 2017b, ApJ, 835, 277
Herwig, F. 2001, ApJ, 554, L71
Hong, K., Lee, J. W., Koo, J.-R., et al. 2021, AJ, 161, 137
Howell, S. B., Sobeck, C., Haas, M., et al. 2014, PASP, 126, 398
Jenkins, J. M., Twicken, J. D., McCauliff, S., et al. 2016, in Proc. SPIE, Vol. 9913, Software and Cyberinfrastructure for Astronomy IV, 99133E
Kawaler, S. D. 1987, in IAU Colloq. 95: Second Conference on Faint Blue Stars, ed. A. G. D. Philip, D. S. Hayes, & J. W. Liebert, 297–307
Kawaler, S. D. 1988, in IAU Symposium, Vol. 123, Advances in Helio- and Asteroseismology, ed. J. Christensen-Dalsgaard & S. Frandsen, 329
Kawaler, S. D. & Bradley, P. A. 1994, ApJ, 427, 415
Koen, C. & Laney, D. 2000, MNRAS, 311, 636
Lightkurve Collaboration, Cardoso, J. V. d. M. a., Hedges, C., et al. 2018, Lightkurve: Kepler and TESS time series analysis in Python
McGraw, J. T., Starrfield, S. G., Liebert, J., & Green, R. 1979, in IAU Colloq. 53: White Dwarfs and Variable Degenerate Stars, ed. H. M. van Horn, V. Weidemann, & M. P. Savedoff, 377–381
Miller Bertolami, M. M. & Althaus, L. G. 2006, A&A, 454, 845
Miller Bertolami, M. M. & Althaus, L. G. 2007a, A&A, 470, 675
Miller Bertolami, M. M. & Althaus, L. G. 2007b, MNRAS, 380, 763
Miller Bertolami, M. M., Althaus, L. G., Serenelli, A. M., & Panei, J. A. 2006, A&A, 449, 313
O'Donoghue, D. 1994, MNRAS, 270, 222
Østensen, R. H., Bloemen, S., Vučković, M., et al. 2011, ApJ, 736, L39
Pych, W. 2004, PASP, 116, 148
Quirion, P. O., Fontaine, G., & Brassard, P. 2007, ApJS, 171, 219
Ricker, G. R., Winn, J. N., Vanderspek, R., et al. 2015, Journal of Astronomical Telescopes, Instruments, and Systems, 1, 014003
Saio, H. 1996, in Astronomical Society of the Pacific Conference Series, Vol. 96, Hydrogen Deficient Stars, ed. C. S. Jeffery & U. Heber, 361
Stanghellini, L., Cox, A. N., & Starrfield, S. 1991, ApJ, 383, 766
Starrfield, S., Cox, A. N., Kidman, R. B., & Pesnell, W. D. 1984, ApJ, 281, 800
Starrfield, S. G., Cox, A. N., Hodson, S. W., & Pesnell, W. D. 1983, ApJ, 268, L27
Tassoul, M., Fontaine, G., & Winget, D. E. 1990, ApJs, 72, 335
Unno, W., Osaki, Y., Ando, H., Saio, H., & Shibahashi, H. 1989, Nonradial oscillations of stars
Wang, K., Zhang, X., & Dai, M. 2020, ApJ, 888, 49
Werner, K. & Herwig, F. 2006, PASP, 118, 183
Werner, K., Rauch, T., & Kepler, S. O. 2014, A&A, 564, A53
Winget, D. E., Hansen, C. J., & van Horn, H. M. 1983, Nature, 303, 781
Winget, D. E. & Kepler, S. O. 2008, ARA&A, 46, 157
Winget, D. E., Nather, R. E., Clemens, J. C., et al. 1991, ApJ, 378, 326